Figure S1. The muscle detachment phenotype observed when the dominant-negative *sdΔTEA* was expressed in *rhea*^{1} mutants was not due to the lack of localization of integrin or its known ligands. **A)** In wild type embryos, Tig (A^1, red) and PS2 integrin (A^2, blue) containing complexes forms a tight junction holding muscles together. (arrowhead in $A^{3'}$). **B)** Tig (B^1, red) and PS2 integrin (B^2 blue) remained concentrated at the muscle cell termini and followed the detaching muscles in *rhea*^{1} embryos where Vg activity is inhibited by *sdΔTEA* (arrows, arrowhead in $B^{3'}$). **C)** Tig (C^1, red) and Tsp (C^2 blue) showed the same localization and retention at the end of detaching muscles in *rhea*^{1} embryos where Vg activity is inhibited (arrows, arrowhead in $C^{3'}$). $A^{3'}$, $B^{3'}$, and $C^{3'}$ are magnifications of the framed areas in A^3, B^3 and C^3 respectively.

Figure S2. Loss of Vg or expression of DN-egfr or over-expression of Vg does not alter tendon cell or specific muscle cell identity. **A)** The pattern of muscles were marked by Myosin (Tadokoro *et al.*) and tendon cells in wild type embryos was visualized by staining of SrA (green), a marker for fully differentiated tendon cells. **B)** $vg^{null};rhea^{1}$ double mutants did not have detectable defects in tendon cell development. **C)** The identity of VL1 muscle can be specifically marked by using a *5053*-GAL4, UAS-*lacZ* marker. **D)** In vg^{null} mutants, VL1 muscles were properly specified at all stages of embryonic development. **E)** The *krüppel*-expressing muscle progenitor cells can be revealed through Kr staining in stage 13 wild type embryos (arrows). **F)** These progenitor cells still express Kr when Vg was over-expressed in SMs via *Dmef2*-GAL4 (arrows). **G)** In wild type embryos, the overall pattern of embryonic muscles can be observed via staining with Myosin (green). The VL1-4 muscles were identified by their position and presence of Vg (Tadokoro *et al.*), LL1 muscles are marked with arrows. **H)** Expression of DN-egfr in the muscles of developing embryos did not alter the specification of the VL muscles but muscles LL1 (arrows) and VO5-6 (arrowheads) were missing in several segments.

Figure S3. The altered migration of LT muscles caused by ectopic-expression of Vg is independent of the Slit-Robo guidance signals and Grip. **A)** The normal pattern of wild type muscles visualized by Actin staining (green). **B)** In embryos with the *robo*^{1} mutation, LT muscles migrated to intrasegmental sites (arrowheads) distant from the segment border (arrow). **C)** A similar pattern of LT muscle migration to intrasegmental sites (arrowheads) distant from the segment border (arrow) as was seen in embryos with the *slit*^{2} mutation. **D)** Ectopic-expression of Vg in wild type embryos caused LTs (arrowheads) to change their apparent migration path and attach to the segment borders (arrows). **E-F)** The *robo*^{1} or *slit*^{2} did not alter this apparent aberrant migration. **G)** In some segments, ectopic-expression of Robo1 produced a phenotype similar to ectopic Vg, with LT1 muscles (arrowheads) moving to the segment borders (arrowheads). **H)** Expression of Robo1 in all developing muscle cells in *vg*^{null} mutant embryos produced a similar phenotype. **I)** Removing *grip* function in muscles cells ectopically expressing Vg did not significantly alter the phenotype induced by over-expression of Vg alone compared to (D).

Figure S4. A-A') The *ap*-GAL4 line induces expression only in muscle LT1-4 and VA2 at similar levels as detected by an UAS-*lacZ* reporter. Dmef2 staining reveals all nuclei of somatic muscles (green). A and A' show different channels of the same cofocal image and so as B and B', C and C'. **B-B')** Expression of UAS-*vg2* via *ap*-GAL4 produced ectopic adhesions between VA2 and LT muscles (arrowheads), but not between VA1 and LT muscles. Insets are the close-ups of the area framed by dotted lines. **C-C')** These ectopic adhesions disappeared when the DN-egfr was co-expressed with Vg (arrowheads).

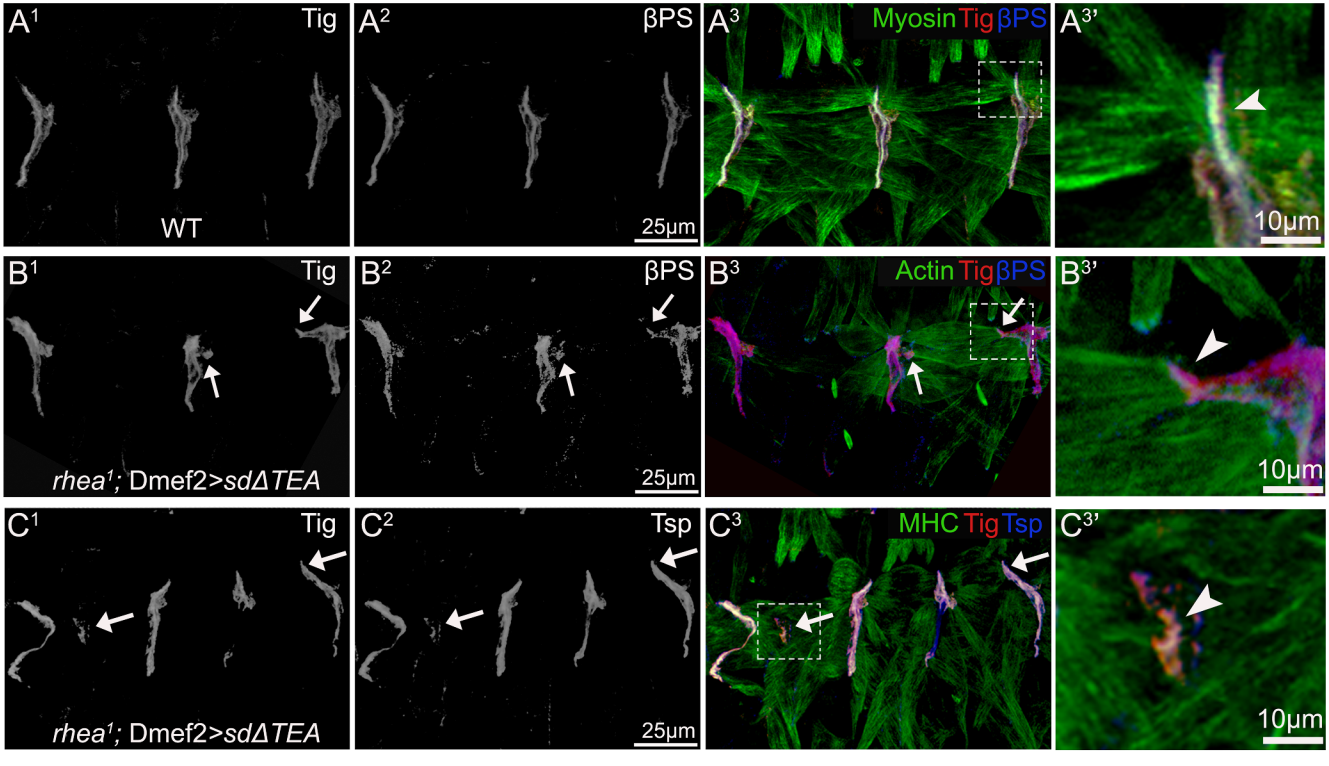
A1
Tig
WT
A2
βPS
25μm
A3
Myosin Tig βPS
A3'
10μm
B1
Tig
rhea1; Dmef2>sdΔTEA
B2
βPS
25μm
B3
Actin Tig βPS
B3'
10μm
C1
Tig
rhea1; Dmef2>sdΔTEA
C2
Tsp
25μm
C3
MHC Tig Tsp
C3'
10μm

Figure S1

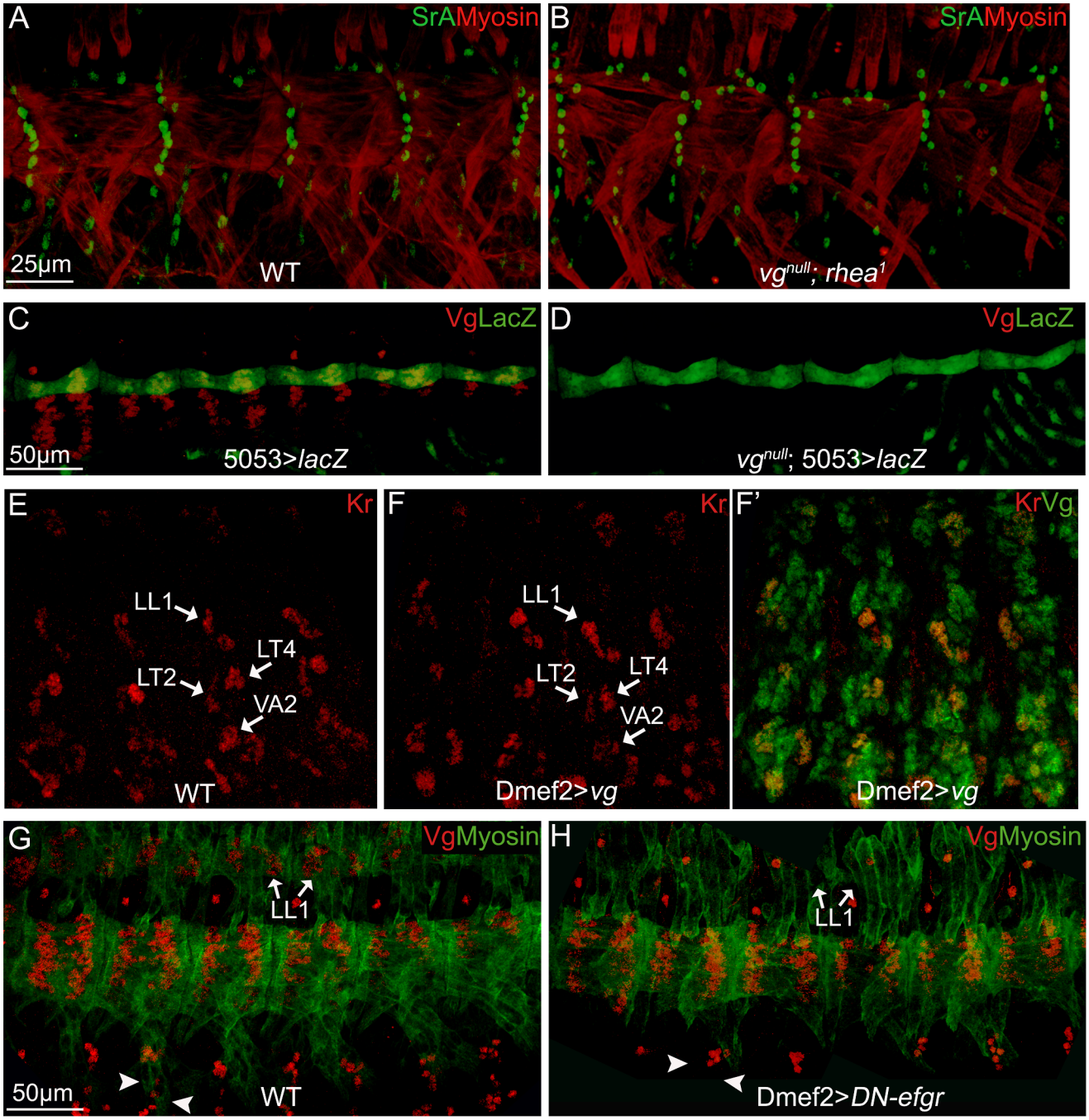
A
SrAMyosin
25µm
WT
B
SrAMyosin
vg^null; rhea^1
C
VgLacZ
50µm
5053>lacZ
D
VgLacZ
vg^null; 5053>lacZ
E
Kr
LL1
LT4
LT2
VA2
WT
F
Kr
LL1
LT2
LT4
VA2
Dmef2>vg
F'
KrVg
Dmef2>vg
G
VgMyosin
LL1
50µm
WT
H
VgMyosin
LL1
Dmef2>DN-efgr

Figure S2

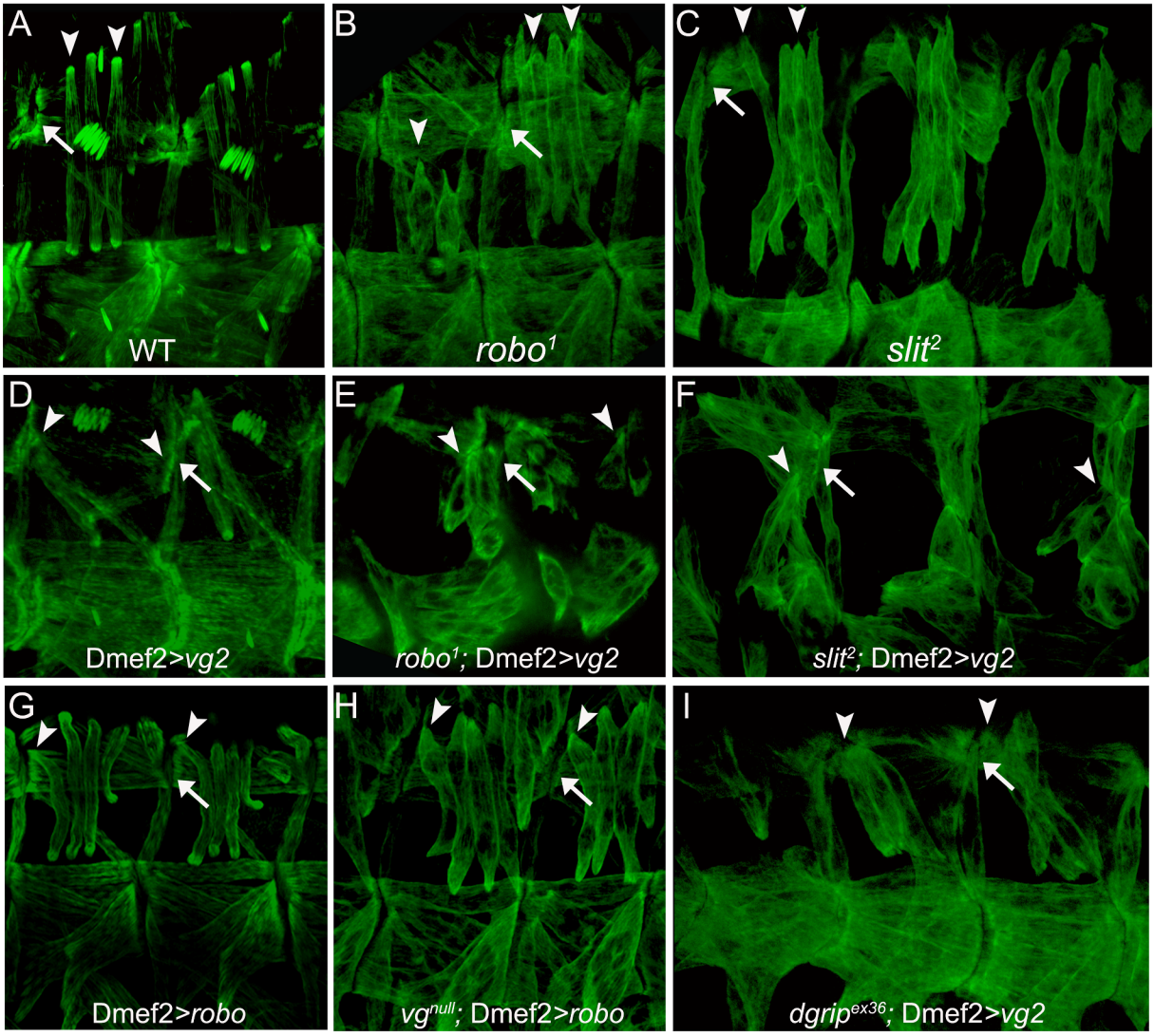
A
WT
B
robo1
C
slit2
D
Dmef2>vg2
E
robo1; Dmef2>vg2
F
slit2; Dmef2>vg2
G
Dmef2>robo
H
vgnull; Dmef2>robo
I
dgripex36; Dmef2>vg2

Figure S3

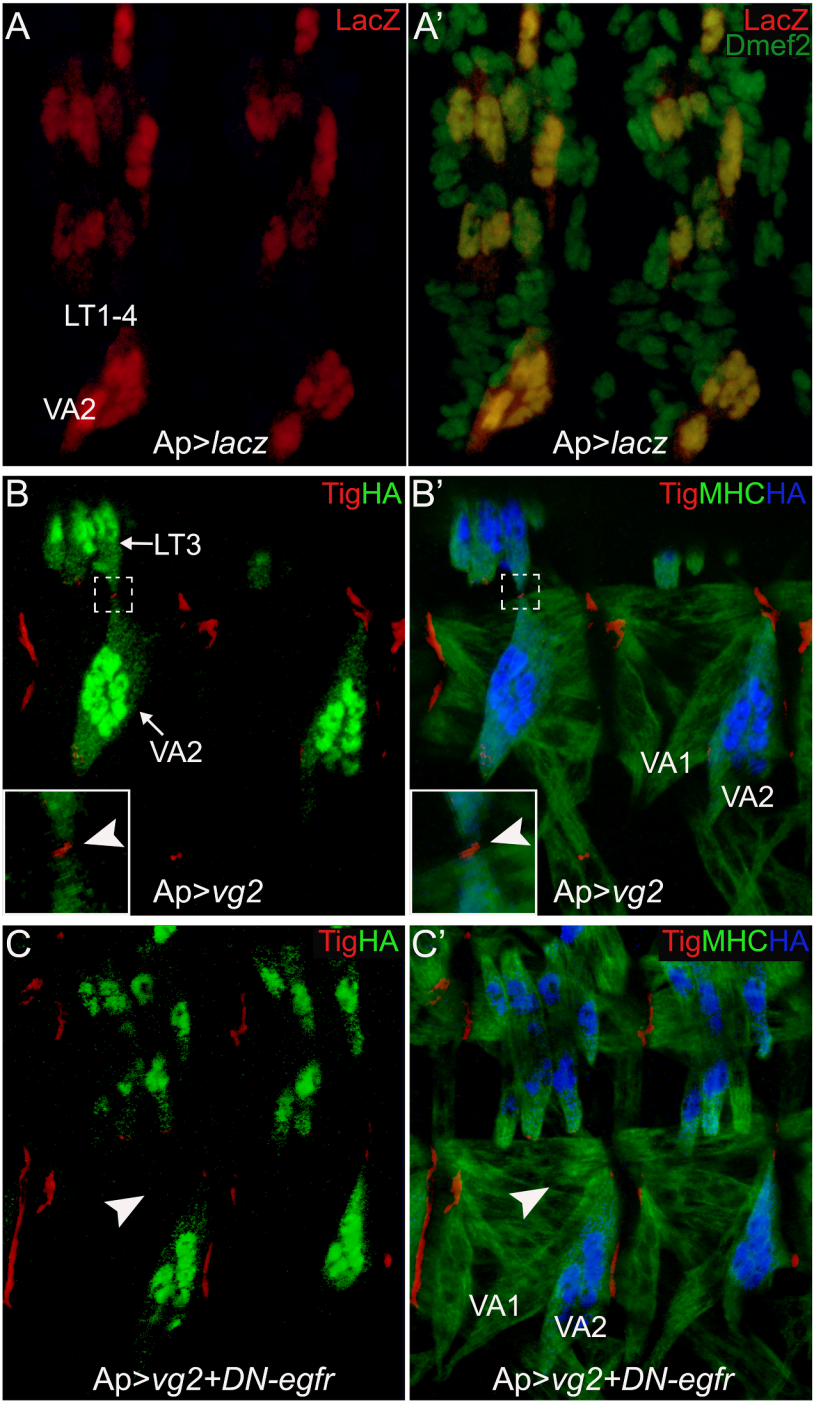
A
LacZ
LT1-4
VA2
Ap>lacz
A'
LacZ
Dmef2
Ap>lacz
B
TigHA
LT3
VA2
Ap>vg2
B'
TigMHCHA
VA1
VA2
Ap>vg2
C
TigHA
Ap>vg2+DN-egfr
C'
TigMHCHA
VA1
VA2
Ap>vg2+DN-egfr

Figure S4